

IMPACT OF FREESTREAM TURBULENCE ON THE BOOM LENGTH

MADUAKO E. OKORIE¹ & Professor FREDDIE L. INAMBAO^{2*}

¹Namibia University of Science and Technology, Windhoek, Namibia. PhD Student, Department of Mechanical Engineering,
University of KwaZulu-Natal, Durban, 4041, South Africa

^{2*}Department of Mechanical Engineering, University of KwaZulu-Natal, Durban, 4041, South Africa

ABSTRACT

Instrumented towers used for wind measurement are in the region of the atmosphere where atmospheric turbulence is expected to dominate the flow regime. Error readings captured by the speed sensors as a result of tower shadowing are expected to increase due to atmospheric turbulence. Although the understanding is that tower shadowing should be considered as an atmospheric rather than an arbitrary external flow problem, key issues are still unknown, such as the influence of freestream turbulence on the boom length needed to keep the anemometer out of tower wake distortions. This study sought to understand the exact effect of freestream turbulence on boom lengths by performing three-dimensional (3D) computational fluid dynamics (CFD) flow simulation around and through the 3D complex geometry of lattice triangular communication towers located at Amper-bo and Korabib in southern Namibia. The impact of freestream turbulence was investigated by comparing the simulation results that capture the site's realistic freestream turbulence parameters to the simulation results obtained from standard external flow analysis (5 % turbulence intensity [TI] and 1 m length scale being the default setting in Ansys fluent) at three heights (10 m, 65 m, and 200 m). The shear stress transport ($k-\omega$ SST) turbulence model that uses the blending function to activate the $k-\omega$ model near the wall, and the $k-\epsilon$ model in the free stream region, were adopted. Flow interferences near the tower wall with the boom length at the desired distance upstream from the tower surface were accurately captured. Results from laminar derived flow distortion using the same wind speeds observed at 10 m, 65 m, and 200 m as reference speeds were compared with the previous two approaches with different turbulence parameters. At Amper-bo, based on the International Electro technical Commission (IEC 6400-12-1) standard boom configuration, at 10 m, 65 m and 200 m, the anemometers should be positioned approximately at 1.6L, 1.9L and 2.3L from the tower surface to achieve 99 %, 99.5 % and 101 % of the freestream velocity, respectively. At Korabib, anemometers should be positioned approximately at 0.7L, 0.9L and 1.3L from the tower surface to achieve 99 %, 99.5 % and 101 % of the freestream velocity, respectively. The results show that freestream turbulence does not have a significant impact on the length of boom needed to keep the anemometer out of the tower wake. Speedup at the tower edges and around individual members was used as a measure of how complex the flow interference was. Higher percentage of speeds were computed at all heights using the simulation parameter that captured the sites' environment, while the laminar model generated the least speedup. Again, the results show that drag on each member of the tower increased with increase in turbulence levels. Finally, it is safe to conclude that freestream turbulence does not have any significant impact on the boom but makes flow interference more complex within the regions near the wall of the tower. It also increases the drag on the tower and engenders visible inhomogeneity in the flow parameters in the wake of the tower.

KEYWORDS: Freestream Turbulence, Boom Length, Drag Coefficient, Speedup & Wind Speed

Received: Jun 01 2021; Accepted: Jun 21, 2021; Published: Jul 20, 2021; Paper Id.: IJMPERDAUG202126

1. INTRODUCTION

Instrumented towers used for wind measurement are in the region of the atmosphere where atmospheric turbulence is expected to dominate the flow regime. Tower shadowing contributes a non-negligible error to anemometer readings. The error is expected to increase if the tower is exposed to atmospheric turbulence. Earliest reported literature (i.e., Cermak, & Horn, 1968; Perrin et al., 2007) opined that turbulence increase does not increase the tower induced flow defect significantly. CFD derived flow distortion was performed on lattice and tubular towers that were modelled as actuator discs (Tusch et al., 2011). The authors reported an increase in tower induced flow distortion due to freestream turbulence increase when compared with International Electrotechnical Commission (IEC) (2005) and IEC (2017). In Fabre et al. (2014), a 3D CFD flow simulation around a complex 3D structure of a lattice triangular tower was performed using $k - \omega SST$ turbulence model in Open FOAM solver (Simple foam). With turbulence intensity (TI) of 5% and length scale (L) calculated as a function of the computational domain, the study showed that tower wake distortion increased due to freestream turbulence when compared with IEC (2005) and IEC (2017). Eidsvik (2014) and Richard and Hoxey (1993) provided a set of equations suitable for modeling atmospheric flow. Furthermore, Lofti (2015) conducted a comparative study on the choice of boundary conditions for modelling atmospheric turbulence. For each of the boundary conditions compared, the author reported an increase in tower wake distortion due to the increased level of turbulence and stated that the approach used in Fabre et al. (2014) leads to under prediction of the boom length at some incident wind angles. The study concluded that tower shadowing should be considered as an atmospheric problem rather than arbitrary external flow problem. Notably, no common approach was adopted for the previous studies. Also, application of the outcomes of previous studies are limited when towers of different configurations, located in different atmospheric conditions in the boundary layer are concerned. On this premise, continuous evaluation is needed, hence this study. This paper sought to understand the exact impact of free stream turbulence on boom length. It was aimed at finding out if it is justified to invest extra resources towards evaluating the phenomenon (tower shadowing) as an atmospheric problem. This vital detail is not found in previous literature. The results of the study will enable stakeholders to make an informed decision on whether or not to invest extra computational costs and other resources in treating tower shadowings as an atmospheric flow problem. Finally, the outcome of this study contributes to literature and further assists stakeholders with required adjustments needed, if any, in order to account for the extra flow perturbations resulting from freestream turbulence influence.

2. BACKGROUND

Amper-bo (25.354°S, 18.313°E) and Schlip (24.030°S, 17.131°E) are the two National Wind Resource Assessment Project (NWRAP) sites selected for this study; they are 1152 m and 1381 m, respectively, above sea level. QinetiQ Ltd (UK) ZephIR Z300 LiDAR was placed near the foot of the instrumented communication towers for wind measurement. The tower construction and instrumentation details are found in Okorie and Inambao (2021a) and Okorie and Inambao (2019). The two tower modules used are equilateral triangular in nature and the construction details are reported in Okorie and Inambao (2021a). The width and height of the tower module at Amper-bo are 1.1 m and 0.89 m, respectively. The tower is constructed with vertical tubular rods (100 mm outer diameter) and a network of angular cross and horizontal bracings. The construction details of the tower at Schlip are the same as the tower at Amper-bo. The tower at Korabib has sharp edges. It has three vertical angle bars (70 mm x 70 mm x 6 mm) and a network of smaller angular cross and horizontal bracings. The width and height of the tower module are 1.320 m and 1.512 m, respectively.

3. GOVERNING EQUATIONS

Fluid flow was governed by the conservation of mass (continuity) and conservation of momentum (RANS equations), shown in Equation 1 and Equation 2, respectively.

$$\frac{\partial \bar{U}_i}{\partial x_j} = 0 \quad 1$$

$$\frac{\partial (\bar{U}_i \bar{U}_j)}{\partial x_j} = -\frac{\partial \bar{P}}{\partial x_i} + \frac{\partial}{\partial x_j} \left\{ \mu_i \left(\frac{\partial \bar{U}_i}{\partial x_j} + \frac{\partial \bar{U}_j}{\partial x_i} \right) - \rho \overline{u'_i u'_j} \right\} \quad 2$$

Where \bar{u} is the Reynolds-averaged velocity, \bar{P} is the averaged pressure, μ is the eddy viscosity and $\overline{u'_i u'_j}$ is the Reynolds stress tensor.

The presence of the stress terms introduces more variables that cannot be fully resolved with the available equations, hence the closure problem. Turbulence models often used in external aerodynamics flow simulations are therefore employed to resolve the closure problem. The shear stress transport (k- ω SST) turbulence model adopted in this study uses the blending function to activate the k- ω model near the wall and k-e model within the freestream region (Fabre et al., 2014). With the chosen turbulence model, complex flow interference and drag near the tower wall are accurately captured.

The equations used are.

$$\frac{\partial (\rho k)}{\partial t} + \frac{\partial (\rho U_i k)}{\partial x_i} = \tilde{P}_k - \beta^* \rho k \omega + \frac{\partial}{\partial x_i} \left[(\mu + \rho_k \mu_t) \frac{\partial k}{\partial x_i} \right] \quad 3$$

$$\frac{\partial (\rho \omega)}{\partial t} + \frac{\partial (\rho U_i \omega)}{\partial x_i} = \alpha \rho S^2 - \beta \rho \omega^2 + \frac{\partial}{\partial x_i} \left[(\mu + \sigma_\omega \mu_t) \frac{\partial \omega}{\partial x_i} \right] + 2(1 - F_1) \rho \sigma_{\omega 2} \frac{1}{\omega} \frac{\partial k}{\partial x_i} \frac{\partial \omega}{\partial x_i} \quad 4$$

According to Fabre et al. (2014), the blending function F_1 is defined by:

$$F_1 = \tanh \left\{ \min \left[\max \left(\frac{\sqrt{k}}{\beta^* \omega y}, \frac{500\nu}{y^2 \omega} \right), \frac{4\rho \sigma_{\omega 2} k}{CD_{K\omega} y^2} \right] \right\}^4 \quad 5$$

4. METHODS

The boundary conditions that capture the sites' realistic freestream turbulence parameters were used during flow simulation. In this regard, two sets of equations proposed by Eidsvik (2014) and Richard and Hoxey (1993) (Table 1) were used to compute the friction velocity (u_*), turbulent kinetic energy (k) and turbulence dissipation rate (ε).

Table 1: Equations for Capturing the Flow Variables.

P.J. Richards and R.J. Hoxey, 1993	Karl J. Eidsvik
$u_* = UK / \ln(z/z_o)$	$u_* = UK / \ln(z/z_o)$
$k = u_*^2 / \sqrt{C_\mu}$	$k = u_*^2 / \sqrt{C_\mu} (1 - z/\delta)^2$
$\varepsilon = u_*^3 / Kz$	$\varepsilon = u_*^3 / Kz (1 - z/\delta)^2$

Notes: where U is the upstream velocity, z is the reference height, z_o is the roughness length, K is Von Karman's constant = 0.4, $C_\mu = 0.09$ and $(\delta = 1000 \text{ m})$ is the boundary layer thickness considered in (Eidsvik, 2008).

Based on the observed wind data, the site representative turbulence intensity was computed. InIEC (2005) the representative turbulence intensity is used to characterize the site's TI. The representative TI is the mean TI plus 1.28 standard deviation of the mean value, calculated from 15 m/s statistics. The representative TI is equal to the 90th percentile of the mean TI values. The turbulence intensity (TI), turbulence length scale (L) and the specific turbulence dissipation rate (ω) were computed using the equations shown in table 2.

Table 2: Recommended Equations for Computation of Turbulence Flow Parameters

$k = 3/2 (\overline{UI})^2$	$\varepsilon = (C_\mu^{0.75} k^{1.5})/l$	$\omega = (C_\mu^{0.75} k^{0.5})/l$
-----------------------------	--	-------------------------------------

5. BRIEF DESCRIPTION OF THE OBSERVED DATA

The observed data analyzed and reported in this work were captured using LiDAR and speed sensors placed on the communication towers at Amper-bo and Schlip. The LiDAR measured data at Amper-bo for a period of 8.4 months (16th Jan. 2014 to 30th Sept. 2014) and approximately 3 months (31st of Sept. to Dec. 2014) at SchlipOkorie and Inambao (2020). The detailed tower instrumentations at different hub heights and mean speeds captured by LiDAR and anemometers mounted on the towers at Amper-bo and Schlip are found in Okorie and Inambao (2020). Apart from the site observed wind speed at each hub height, the roughness length is another parameter that plays a pivotal role in estimation of the friction velocity (u^*) needed to compute the turbulent kinetic energy (k) and the turbulent dissipation rate (ε). A multi-point fitted log law approach was adopted for computation of the z_0 and the result from both measurement techniques at both sites are summarized in Table 3. The mean and peak values of z_0 obtained from the in-situ measurement were used in this study because the mean value captures the seasonal variation of z_0 , and the monthly peak values indicate the maximum z_0 obtained from the sites (Table 3).

Table 3: Summary of the Mean and Peak values of z_0 of at Amper-bo and Schlip in 2014

	Amper-bo		Schlip	
	Mean Value of z_0 (Annual-2014)	Peak Value of z_0 (June-2014)	Mean Value of z_0 (Annual-2014)	Peak Value of z_0 (June-2014)
Anemometers	0.494	1.51	0.0397	0.139
	Mean value of z_0 for 8.4 months	Peak value of z_0 (June-2014)	Mean value of z_0 for 3 months	
LiDAR	0.626	1.06	0.0243	-

6. RESULTS AND DISCUSSIONS

6.1 TI and Length Scale Variations with Heights

Based on the models proposed in Eidsvik (2008) and Richards and Hoxey (1993), the friction velocity (u^*), turbulence kinetic energy (k), and the rate of dispersion of turbulence kinetic energy (ε) were computed. Inputting these parameters in the set of equations in table 2, the TI, length scale (L), and turbulence dispersion rate (ω), were obtained. The TI values obtained from Eidsvik (2008) and Richards and Hoxey (1993), equations were compared to the mean and representative TI values obtained from the observed wind data. From Figure 1 it is evident that the TI values generally decrease with height at both sites, as expected. The computed TI values based on Eidsvik (2008) and Richards and Hoxey (1993) equations predicted accurately the sites' mean TI values.

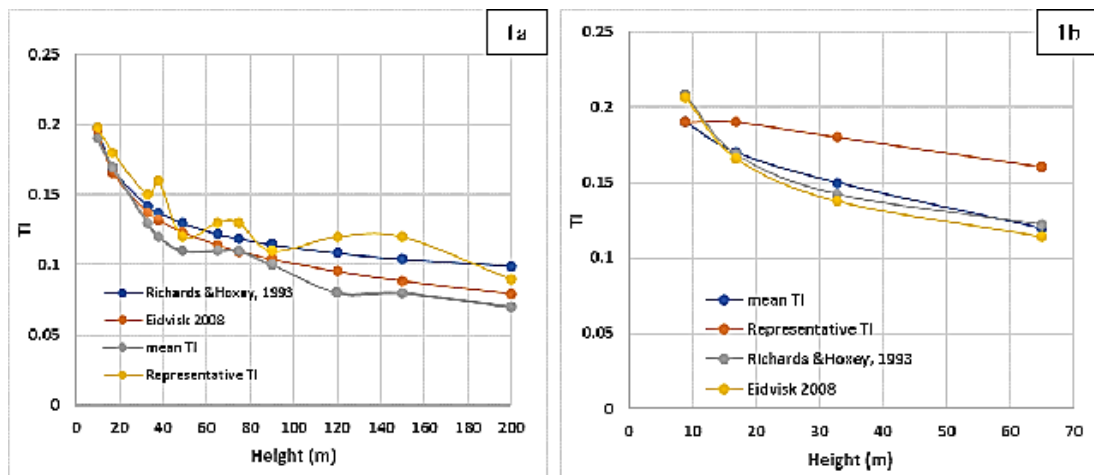


Figure 1a: Calculated TI as Function of Height for the LiDAR Observed Data at Amper-bo.

Figure 1b: Calculated TI as a Function of Height for the in-Situ Measurement at Amper-bo.

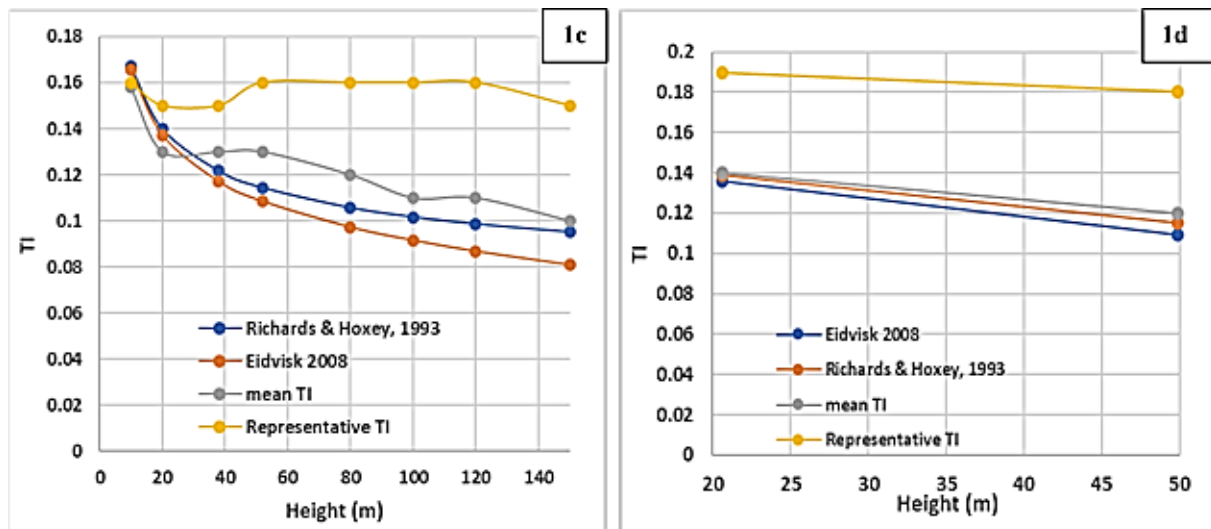


Figure 1c: Calculated TI as Function of Height for LiDAR Data Observed at Schlip.

Figure 1d: Calculated TI as a Function of Height for in-Situ Measured data at Schlip.

The representative TI values were higher than the rest at both sites and with both measurement techniques. The representative TI values were therefore used with other relevant parameters from the sites to calculate the length scale and turbulence dispersion rate. In general, the length scale increased with height (Figure 2) while turbulence dispersion rate (ω) decreased with height. Figures 2a and 2b illustrate the length scales drawn as a function of height for both the LiDAR observed and the in-situ measurement at Amper-bo. Also, Figures 2b and 2c show the variation of the length scale with height for LiDAR and in-situ observed data at Schlip. For both measurement techniques, and at both sites, the length scale computed using the representative TI is higher than the values predicted by Eidsvik (2008) and Richards and Hoxey (1993), models and was more pronounced at Schlip. The over prediction of the length scale at other heights when the representative TI was used as the input parameter was expected, as the representative TI value was obtained at 15 m/s. As a result, Richards and Hoxey (1993) which predicted highest values of TI and length scale among the two models, was adopted and used as simulation parameters.

Freestream turbulence impact was investigated by comparing the simulation results that captured the site's realistic freestream turbulence parameters to the simulation results obtained from standard external flow simulation (5 % turbulence intensity (TI) and 1 m length scale in Ansys default) at three heights (10 m, 65 m, and 200 m). Results from laminar derived flow distortion using the same wind speeds observed at 10 m, 65 m and 200 m as reference speeds were compared with the previous two flow simulations with different turbulence parameters.

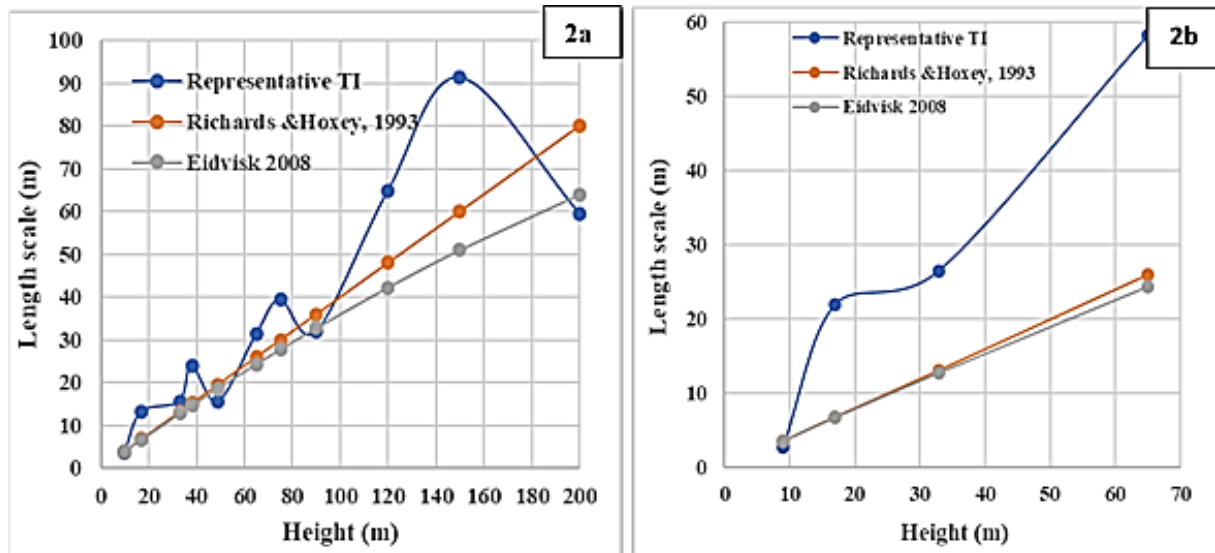


Figure 2a: Calculated Length Scale as a Function of Height for the LiDAR Observed Data at Amper-bo.
Figure 2b: Calculated Length Scale as a Function of Height for the in-Situ Measurement at Amper-bo.

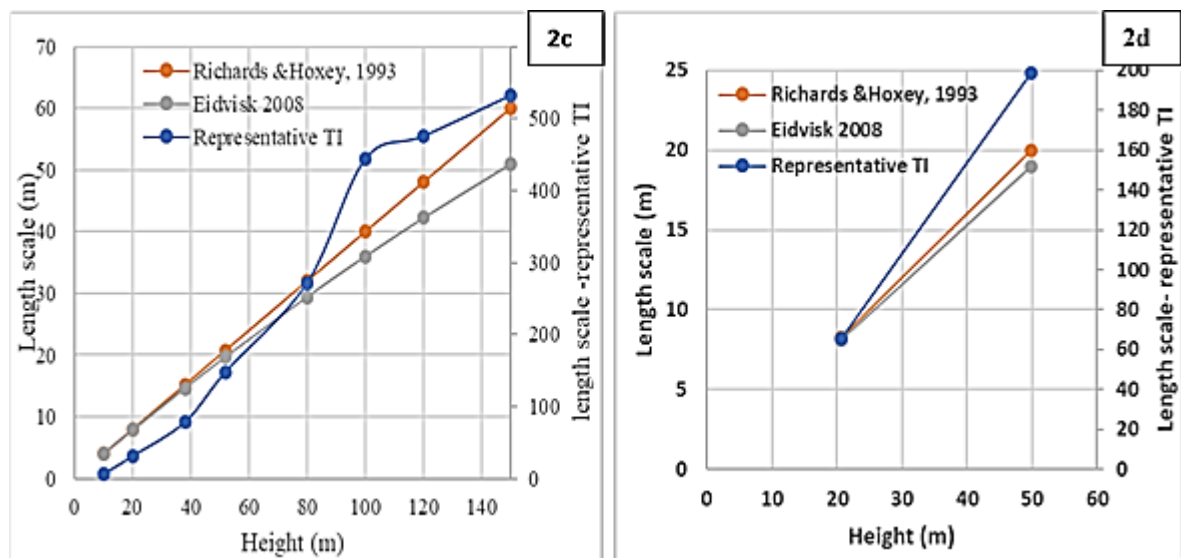


Figure 2c: Calculated Length Scale as a Function of Height for the LiDAR Observed Data at Schlip.
Figure 2d: Calculated Length Scale as a Function of Height for the in-Situ Measurement at Schlip.

6.2 Anemometer Separation Distance from the Tower

Evaluation of the freestream turbulence effect on anemometer separation distance from the tower surface, preferably referred to as the boom length, was the major objective of this paper. Figure 3a is the CFD derived flow distortion over the tower at Amper-bo. The boom length drawn as a function of the normalised velocity from the upstream contour, is

illustrated in figures 3b, 3c and 3d.

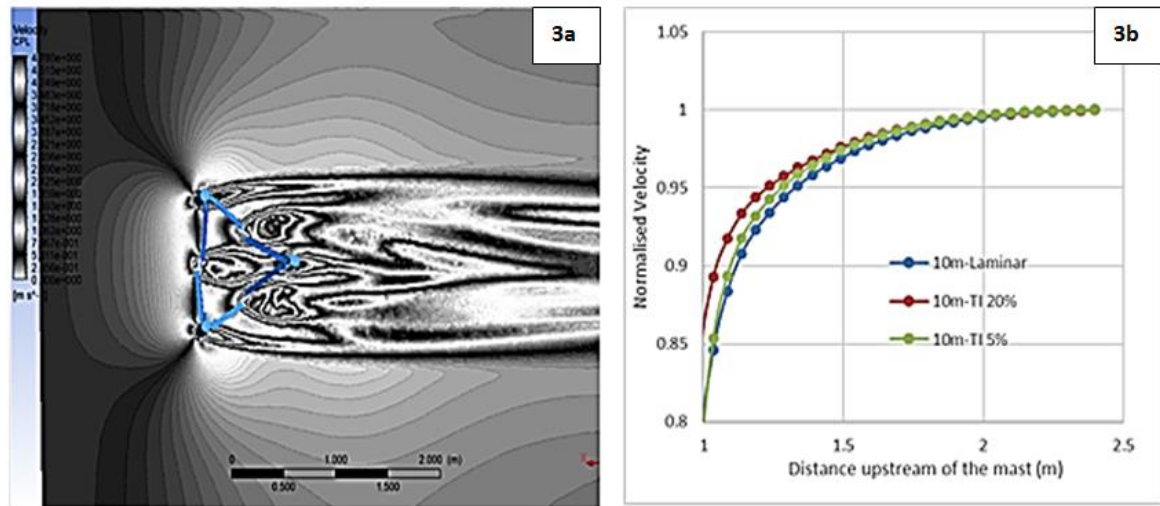


Figure 3a: A 3D CFD Derived Flow Distortion Around the Lattice Triangular Tower at Amper-bo. Figure 3b: The Boom Length from the Tower Surface Drawn as a Function of the Normalised Velocity at 10 m Hub Height of the Tower at Amper-bo.

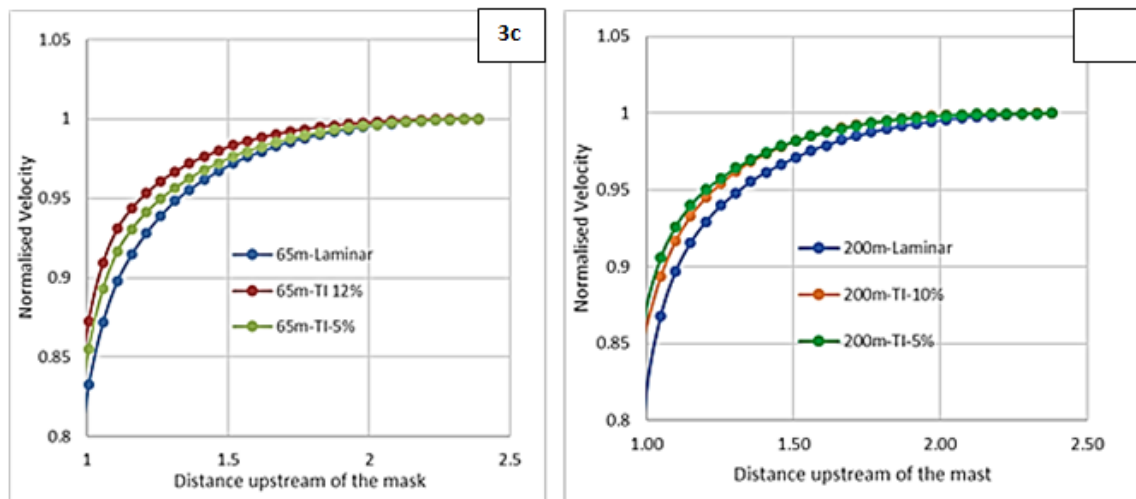


Figure 3c: The Boom Length from the Tower Surface Drawn as a Function of the Normalised Velocity at 65 m Hub Height based on the Tower at Amper-bo. Figure 3d. The Boom Length from the Tower Surface Drawn as a Function of the Normalised Velocity at 65 m Hub Height based on the Tower at Amper-bo.

The boom lengths computed are based on the IEC 6400-12-1 standard boom configuration, where the incident wind is assumed to be perpendicular to the tower face, giving rise to a velocity deficit value that is computed using the upstream contour profile, along the same axis with the incoming winds.

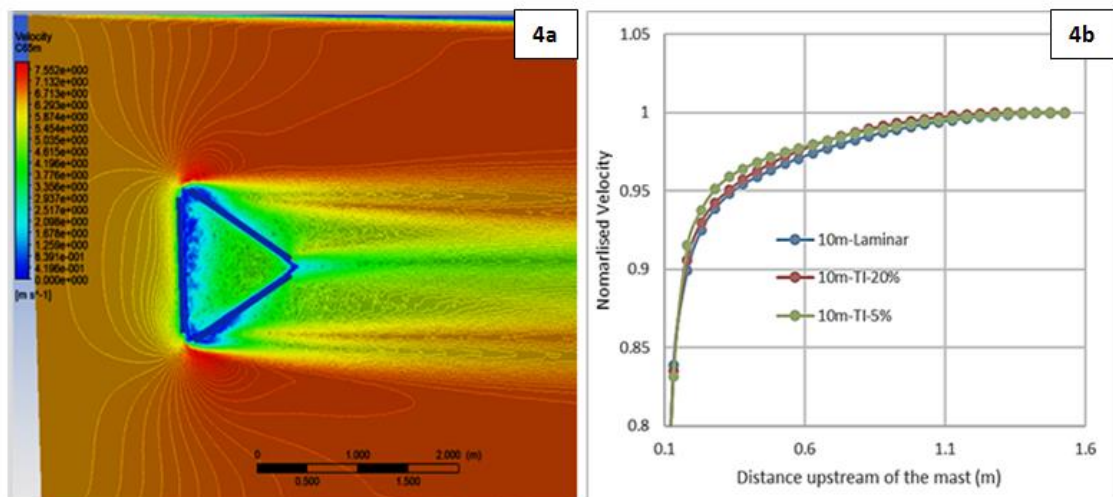


Figure 4a: A 3D CFD Derived flow Distortion around the Lattice Triangular Tower at Korabib.
Figure 4b: The Boom Length from the Tower Surface Drawn as a Function of the Normalised Velocity at 10 m Hub Height of the Tower at Korabib.

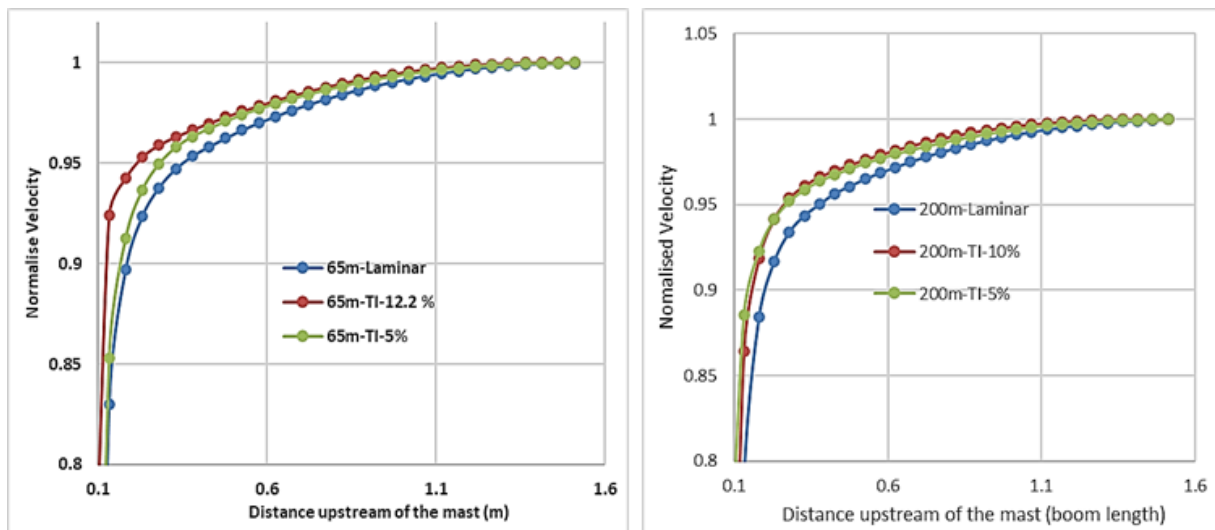


Figure 4c: The Boom Length from the Tower Surface Drawn as a Function of the Normalised Velocity at 65 m Hub Height based on the Tower at Korabib.
Figure 4d: The Boom Length from the Tower Surface Drawn as a Function of the Normalised Velocity at 65 m Hub Height based on the Tower at Korabib.

At Amper-bo the observed wind speeds were 3.7 m/s, 6.3 m/s and 7.5 m/s, at 10 m, 65 m, and 200 m, respectively. For the standard external flow, TI and length scale were 5% and 1 m respectively in Fluent solver. At 10 m height, the calculated TI was 20 %, and the length scale was 4 m. At 65 m height, the calculated TI reduced to 12 % while the length scale increased to 26 m. A further reduction of calculated TI to 10% and a length scale increase of 80 m was computed at 200 m. At the three heights considered, the laminar model appears to produce a more conservative result in the regions very close to the tower wall. The result obtained from the three sets of flow modelling approaches appears to achieve some sort of parity within the region of interest, i.e., at some distance away from the tower surface. The CFD derived flow simulation that captures the realistic site freestream turbulence, the standard external flow approach(5% TI and 1 m length scale) and their laminar counterparts predicted approximately the same boom length. At 10 m, 65 m and 200

m, anemometers should be positioned approximately at 1.6L, 1.9L and 2.3L from the tower surface to achieve 99 %, 99.5 % and 101 % respectively of the freestream velocity.

Again, similar flow modelling approaches and boundary conditions were used on the tower at Korabib (which has sharp edges). The laminar model also appears to produce a more conservative result in the regions nearer to the tower wall, though insignificant since there was no difference in the boom length reported within the region of interest. With this tower configuration (Figure 4), the three flow modelling approaches used at 10 m, 65 m and 200 m are illustrated in Figures 4b, 4c and 4c. Again, anemometers should be positioned approximately at 0.7L, 0.9L and 1.3L from the tower surface to achieve 99 %, 99.5 % and 101 % of the freestream velocity, respectively. The results obtained from the two towers of different configurations, using different simulation parameters, shows that freestream turbulence does not have a significant impact on the boom length required to keep the speed sensors out of the wake distortion effect of the tower. It is noted that the boom length obtained from this computational approach was more conservative when compared to its counterpart as obtained from the centreline velocity deficit expression described in IEC (2017) and Okorie and Inambao (2021a). However, the difference may not be attributed to the effect of freestream turbulence but rather to the numerical approach, coupled with the oversimplification of the complex 3D nature of an operational tower to a 2D actuator disc model. As reported in Okorie and Inambao (2021b), proper instrumentation of the tower to reduce its shadowing effects requires a combination of physical and numerical modelling, a good understanding of the safe angle range for boom installation, and the prevailing wind pattern on the site.

6.3 Complex Flow Interference and Drag Coefficient

How complex the flow interference around an operational tower is, attributed to its discrete members (IEC, 2017; Okorie and Inambao, 2021a) i.e., horizontal bracings, cross bracings, and other secondary support structures unique to the parent tower's application. Complex flow interference in this context was ascertained by computing the maximum speed-ups at the edges and around other tower discrete members. Regarding the Amper-bo tower, at 10 m height, speed-ups of 34.6 %, 30.2 % and 29.2% were computed from the CFD derived flow distortion when TI of 20 %, TI of 5 % and the laminar models, respectively, were used as the computational parameters. Similarly, at 65 m, speed-ups of 31.1 %, 29.1 % and 27.5 % were obtained from the computation when TI of 12 %, TI of 5 % and the laminar models, respectively, were used. At 200 m height, 30.3 %, 28.9 % and 26.4 % were speed-ups computed from the CFD derived flow distortion when TI of 10 %, TI of 5 % and the laminar models, respectively were used as the computational parameters. Regarding the Korabib tower with sharp edges, at 10 m 30.2 %, 28.6 % and 26.5 % were obtained when TI of 20 %, TI of 5 % and the laminar models, respectively, were used as the computational parameters. Similarly, at 65 m, 28.6%, 27.5 % and 25.5 % respectively, were obtained when TI of 12 %, TI of 5 % and the laminar models, respectively, were used as the computational parameters. For similar computational parameters but for TI of 10%, at 200m, 27.4 %, 26.5 % and 24.3 % were obtained. The percentage speed-up values obtained from the three computational approaches differed. Higher percentage speed-ups were evident using the flow parameters that captured the site's realistic freestream turbulence, followed by the standard external flow approach (5% TI and 1 m turbulence length scale in Ansys fluent) and then the laminar model. The TI and speed-up values decreased with height. The results show that the flow interference was much more complex within the regions close to the tower wall due to the freestream turbulence effect. The percentage difference in speed-ups at each height using different simulation parameters was remarkable. Using Amper-bo tower, the percentage difference was approximately 14.1 % and approximately 11.8% with the Korabib tower, on the average. Though not an area of interest in this study, there was

notable inhomogeneity and a large spread of the flow parameters in the wake as result of freestream turbulence. It may be necessary to ascertain the impact of freestream turbulence on boom vibration and its associated errors in relation to the wind speed captured by the speed sensor. This remains a grey area for further research work since complex flow interference is evidently high within the regions that are very close to the tower surface.

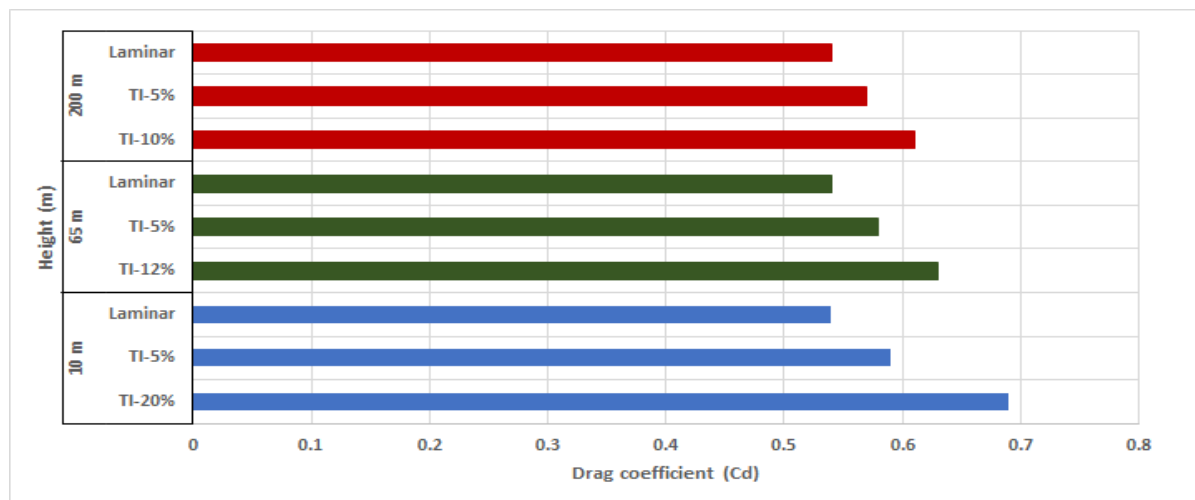


Figure 5: The Drag Coefficients (Cd) based on CFD Flow Simulation Around the Tower at Amperbo using TI and Length Scales Values Computed at Different Heights.

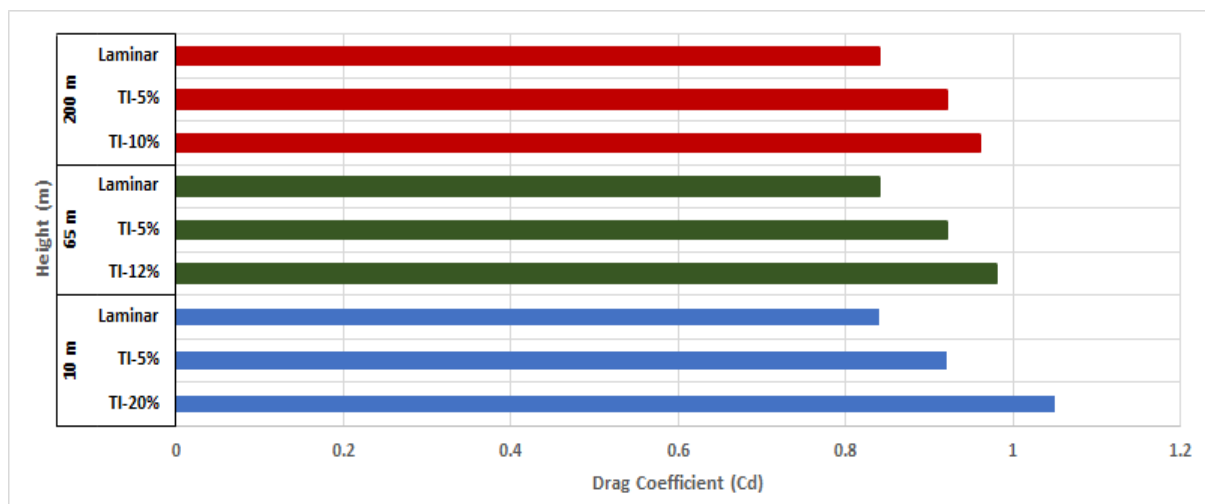


Figure 6: The Drag Coefficients (Cd) based on CFD Flow Simulation Around the Tower at Korabib using TI and Length scales Values Computed at Different Heights.

Figure 5 and Figure 6 are the drag coefficients drawn as a function of the height. The drag coefficient (Cd) obtained from laminar flow over the Amper-bo tower module was approximately 0.54 at all heights whereas a Cd of approximately 0.84 was recorded for the tower at Korabib. Again, based on the standard external flow approach (5% TI and 1 m length scale in Ansys fluent), Cds of approximately 0.59 and 0.92 were computed at all heights using the Amper-bo and Korabib tower modules, respectively. When the simulation parameters that captured the sites realistic freestream turbulence at the three heights were used, Cd values that were somewhat related to the TI values were obtained. Using the tower module at Amper-bo, Cd was 0.69 when TI was 20% at 10 m height, while it was 0.63 for TI value of 12 % at 64 m. At 200 m, Cd was 0.61 when TI was 10%. The Cd computed at 10 m height was 9.5 % and 11.6% higher than the values

obtained at 65 m and 200 m, respectively.

Similarly, using the tower module at Korabib, C_d was 1.05 when TI was 20% at 10 m height, while it was 0.98 for TI value of 12 % at 64 m. At 200 m, C_d was 0.96 when the TI was 10%. The C_d computed at 10 m height was 6.7 % and 8.9% higher than the values obtained at 65 m and 200 m, respectively. Applying the true site freestream characteristics leads to a higher value of C_d when compared to the standard external flow approach and the laminar model. Again, the result showed that increased levels of turbulence increase drag on the individual members of the tower.

7. CONCLUSIONS

A 3D CFD simulation was performed around two lattice equilateral triangular tower modules of different configurations in order to evaluate the impact of atmospheric turbulence on the boom length needed to keep the anemometer out of the wake distortion effect of the tower. Freestream turbulence impact was investigated by comparing the simulation results that captured the site's realistic freestream turbulence parameters to the simulation results obtained from standard external flow analysis (5 % turbulence intensity [TI] and 1 m length scale in Ansys fluent) at the three heights (10 m, 65 m, and 200 m) considered. The shear stress transport ($k - \omega SST$) turbulence model that used the blending function to activate the $k - \omega$ model near the wall, and the $k - \epsilon$ model within the freestream region, were adopted. With the chosen turbulence model, complex flow interference and drag near the tower wall and the boom length at a desired distance upstream from the tower surface were accurately captured. Conclusions based on the derived flow distortion around the towers due to variation of the simulation parameters were as follows:

- The three modelling approaches which hinged on the variation of the CFD simulation parameters, predicted approximately the same length of boom that will keep the speed sensor out of the wake influence of the tower. At 10 m, 65 m and 200 m, anemometers should be positioned approximately at 1.6L, 1.9L and 2.3L from the tower surface to achieve 99 %, 99.5 % and 101 % respectively of the freestream velocity for the tower at Amper-bo. Similarly, at Korabib, anemometers should be positioned approximately at 0.7L, 0.9L and 1.3L from the tower surface to achieve 99 %, 99.5 % and 101 % of the freestream velocity, respectively. The study concludes that atmospheric turbulence does not have a significant impact on the boom length required to keep the speed sensors out of the wake distortion effect of the tower.
- The maximum speed-ups at the edges and around other tower discrete members were evaluated to gain insight into how complex the flow interference was within the vicinity of the towers. First, the study noted that this phenomenon was tower dependent. Second, there was evidence that flow interference was more complex due to atmospheric turbulence. Turbulence intensity decreased with height, as did the percentage speed-ups, irrespective of higher wind speed measured at such higher heights. The percentage difference in speed-ups at each height using different simulation parameters was remarkable. At Amper-bo tower the percentage difference was approximately 14.1 % and at Korabib tower it was approximately 11.8%. Notable inhomogeneity and large spread of the flow parameters in the wake as result of freestream turbulence were evident. Though it has no effect on the computed boom length, nonetheless, it may be necessary to ascertain the impact of freestream turbulence on boom vibration and its associated errors in relation to the wind speed captured by the speed sensor. This remains a grey area for further research work since flow interference appears more complex within the regions that are very close to the tower surface.
- The drag coefficients computed using different simulation parameters show that drag on the tower structures

increased due to atmospheric turbulence; hence the higher values of drag coefficients reported when the turbulence level was high.

Finally, this study investigated the effect of atmospheric turbulence on the boom length by using different simulation parameters to perform a 3D CFD flow analysis around two lattice triangular towers with different construction details. There is evidence that flow interference was more complex within the regions nearer to the tower wall due to the increase in turbulence levels. Drag on each member of the tower increased with increase in turbulence levels as well. However, the study concluded that atmospheric turbulence did not increase the length of booms needed to keep the speed sensor out of the tower wakes.

REFERENCES

1. Cermak, J. E. & J. D. Horn, J. E. (1968). *Tower shadow effect*. *Journal of Geophysical Research (1896-1977)*, 73(6), 1869–1876. doi: 10.1029/JB073i006p01869.
2. Eidsvik, K. (2008). *Prediction errors associated with sparse grid estimates of flows over hills*. *Boundary-Layer Meteorology*, 127, 153–172. doi: 10.1007/s10546-007-9247-9.
3. Fabre, S., Stickland, M., Scanlon, T., Oldroyd, A., Kindler, D., & Quail, F. (2014). *Measurement and simulation of the flow field around the FINO 3 triangular lattice meteorological mast*. *Journal of Wind Engineering and Industrial Aerodynamics*, 130, 99–107. doi: 10.1016/j.jweia.2014.04.002.
4. International Electrotechnical Commission (IEC), (2005). *Wind turbines - Part 1: Design requirements*. International Standard IEC 61400-1:2005(E), Geneva, Switzerland: IEC.
5. International Electrotechnical Commission (IEC), (2005). *Wind energy generation systems – Part 12-1: Power performance measurements of electricity producing wind turbines*. International Standard IEC 61400-12-1:2005(E). Geneva, Switzerland: IEC.
6. International Electrotechnical Commission (IEC). (2017). *Wind energy generation systems – Part 12-1: Power performance measurements of electricity producing wind turbines*. International Standard IEC 61400-12-1:2017-03(en-fr) Accessed: Oct. 15, 2018. [Online]. Available: <https://webstore.iec.ch/publication/26603>
7. Lofti, M. F. (2015). *Atmospheric wind flow distortion effects of meteorological masts*. Master's dissertation, University of Porto, Porto, Portugal, 2015.
8. Okorie, M. E. & Inambao F. L. (2021b). *Local wind flow modifications within the vicinity of a communication tower* *International Journal of Mechanical and Production Engineering Research and Development*, 11(3), 421–440. doi: 10.24247/ijmperdjun202135.
9. Okorie, M. E. & Inambao, F. L. (2020). *Prediction of the impact of tower shading on resource parameters and performance by using LiDAR*. *Building Services Engineering Research and Technology*, 13(11), 3125-3144.
10. Okorie, M. E., & Inambao, F. L. (2019). *Identification of tower and boom wakes using collocated anemometers and Lidar measurement*. *International Journal of Mechanical Engineering and Technology*, 10(6), 72–94.
11. Okorie, M. E., & Inambao, F. L. (2021a). *Angle dependence of tower wake distortion: A parametric study*. *International Journal of Mechanical and Production Engineering Research and Development*, 11(3), 481-498
12. Perrin, D., McMahon, N., Crane, M., Ruskin, H. J., Crane, L., & Hurley, B. (2007). *The effect of a meteorological tower on its top-mounted anemometer*. *Applied Energy*, 84, 413–424.

13. Richards, P. J., & Hoxey, R. P. (1993). Appropriate boundary conditions for computational wind engineering models using the $k-\epsilon$ turbulence model. *Journal of Wind Engineering and Industrial Aerodynamics*, 46–47, 145–153. doi: 10.1016/0167-6105(93)90124-7.
14. Tusch, M., Masson, C., & Héraud, P. (2011). Modeling of turbulent atmospheric flow around tubular and lattice meteorological masts, *Journal of Solar Energy Engineering*, 133(1), 011011. doi: 10.1115/1.4003293.
15. Parmar, Jigar K., Sunny K. Darji, and Gajendra R. Patel. "Fuzzy Based MPPT Controller of Wind Energy Conversion System using PMSG." *International Journal of Electrical and Electronics Engineering (IJEET)* 7.3: 17-30.
16. Isaac, Ann Maria, and K. Rathi. "Performance Analysis of Hybrid HVDC Transmission Systems for Connecting Offshore Wind Farm to Onshore Grid." *International Journal of Innovative Research in Science, Engineering and Technology* 3.5:201-207.
17. Jai Kumar Sharma, Aman Goyal, Mukesh Pandey & Sateesh Kumar, "Design and Analysis of Vertical Axis Wind Turbine Booster at Low Wind Speed", *International Journal of Mechanical and Production Engineering Research and Development (IJMPERD)*, Vol. 10, Issue 3, pp, 13823-13836.
18. S. Sivabalan, G. Sathishkumar, S. Sivaganesan & S. Raja, "Aerodynamic Analysis of Horizontal Axis win Turbine Blade for Low Wind Condition", *International Journal of Mechanical and Production Engineering Research and Development (IJMPERD)* ISSN (P): 2249-6890; ISSN (E): 2249-8001 Special Issue, pp, 316-328

